

Cepheids in external galaxies. I. The maser-host galaxy NGC 4258 and the metallicity dependence of P - L and P - W relations

G. Bono^{1,2}, F. Caputo¹, G. Fiorentino³, M. Marconi⁴, I. Musella⁴

ABSTRACT

We perform a detailed analysis of Cepheids in NGC 4258, Magellanic Clouds and Milky Way in order to verify the reliability of the theoretical scenario based on a large set of nonlinear convective pulsation models. We derive Wesenheit functions from the synthetic BVI magnitudes of the pulsators and we show that the sign and the extent of the metallicity effect on the predicted Period-Wesenheit (P - W) relations change according to the adopted passbands. These P - W relations are applied to measured BVI magnitudes of NGC 4258, Magellanic and Galactic Cepheids available in the literature. We find that Magellanic and Galactic Cepheids agree with the metallicity dependence of the predicted P - W relations. Concerning the NGC 4258 Cepheids, the results strongly depend on the adopted metallicity gradient across the galactic disc. The most recent nebular oxygen abundances support a shallower gradient and provide a metallicity dependence that agrees well with current pulsation predictions. Moreover, the comparison of Cepheid distances based on VI magnitudes with distance estimates based on the revised TRGB method for external galaxies, on the HST trigonometric parallaxes for Galactic Cepheids, and on eclipsing binaries in the Magellanic Clouds seems to favor the metallicity correction predicted by pulsation models. The sign and the extent of the metallicity dependence of the Period-Wesenheit and of the Period-Luminosity relations change according to the adopted passbands. Therefore, distances based on different methods and/or bands should not be averaged. The use of extragalactic Cepheids to constrain the metallicity effect requires new accurate and extensive nebular oxygen measurements.

¹INAF – Osservatorio Astronomico di Roma, Via Frascati 33, 00040, Monte Porzio Catone, Italy

²European Southern Observatory, Karl-Schwarzschild-Str. 2, 85748 Garching bei Munchen, Germany

³Kapteyn Astronomical Institute, University of Groningen, Postbus 800, 9700 AV Groningen, the Netherlands

⁴INAF – Osservatorio Astronomico Di Capodimonte, Via Moiariello 16, 131 Napoli, Italy.

Subject headings: Distance Scale - Classical Cepheids - galaxies: individual (NGC 4258)

1. Introduction

The Period-Luminosity (P - L) relation of Classical Cepheids is a yardstick in several astrophysical and cosmological problems. The Cepheid distances to external galaxies rely on fiducial P - L relations based on Large Magellanic Cloud (LMC) variables and these distance determinations are used to calibrate secondary distance indicators, and in turn to estimate the Hubble constant H_0 . However, a general consensus on the “universality” of the P - L relations, and in particular on their dependence on the Cepheid chemical composition has not been reached yet.

On the theoretical side, it is worth mentioning that the nonlinear convective pulsation models computed by our group (Fiorentino et al. 2007, hereinafter [F07]; Caputo 2008, and references therein) show that the metallicity effect on the predicted P - L relations depends on the adopted photometric band. The synthetic linear P - L relations, for an increase in the global metal content from $Z=0.004$ to 0.02 , become on average shallower, with the slope of the optical P - L_B , P - L_V and P - L_I relations decreasing from $\sim 29\%$, to 15% and to 8% , respectively. The same change in metallicity causes no significant effect on the near-infrared P - L relations. Moreover, quoted predictions also indicate that the metal-rich pulsators with periods longer than five days present *fainter* optical magnitudes than the metal-poor ones. The extent depends once again on the adopted passband. At even larger metal abundances $Z=0.03$ - 0.04 , the pulsation models suggest that the helium content Y also affects the Cepheid properties at periods longer than about ten days. It was also suggested (Fiorentino et al. 2002, hereinafter [F02]; Marconi, Musella & Fiorentino 2005, hereinafter [M05]) that the metallicity effect on Cepheid distances *based on V and I magnitudes*, is not linear over the entire metallicity range $Z=0.004$ - 0.04 , but presents a sort of “turnover” at roughly solar chemical composition. As a whole, the use of LMC-calibrated P - L_V and P - L_I relations to provide distance estimates with an intrinsic error of ± 0.10 mag is fully justified for Cepheids with $P \leq 10$ days and/or helium-to-hydrogen enrichment ratio $\Delta Y/\Delta Z \leq 2.0$ (see e.g. F02 and M05 for more details). On the other hand, the average correction for Cepheids with $P > 10$ days, high metal abundances ($Z \geq 0.03$) and $\Delta Y/\Delta Z \geq 3.0$ is larger than 0.1 mag. As a consequence, Cepheids with $P \geq 20$ days and oxygen abundance¹ $[O/H] \geq 0.2$, as measured

¹According to the conventional logarithmic scale of stellar chemical abundances, for two different elements x_i and x_j one has $[x_i/x_j]=\log(x_i/x_j)_* - \log(x_i/x_j)_\odot$.

in several spiral galaxies observed by the *HST* Key Projects (Freedman et al. 1994; Saha et al. 1994), the average metallicity correction varies from about -0.2 mag to $\sim +0.25$ mag as the adopted $\Delta Y/\Delta Z$ ratio varies from 2 to 3.5.

On the observational side, independent investigations suggest either a negligible metallicity effect or that Galactic (metal-rich) Cepheids are somehow *brighter*, at fixed period, than LMC (metal-poor) variables (Sasselov et al. 1997; Kennicutt et al. 1998, 2003; Kanbur et al. 2003; Tammann et al. 2003; Sandage et al. 2004; Storm et al. 2004; Groenewegen et al. 2004; Sakai et al. 2004; Ngeow & Kanbur 2004; Pietrzynski et al. 2007). In the latter case, the empirical metallicity dependence of the Cepheid true distance modulus μ_0 , as usually described by the parameter $\gamma = \delta\mu_0/\delta\log Z$ where $\delta\mu_0$ is the extent of the metallicity correction and $\delta\log Z = \log Z_{LMC} - \log Z_{Ceph}$, spans a large range of *negative* values up to $\gamma = -0.4$ mag dex $^{-1}$, with an average value of approximately -0.25 mag dex $^{-1}$ (Sakai et al. 2004 and references therein). However, spectroscopic iron-to-hydrogen [Fe/H] measurements of Galactic Cepheids (Romaniello et al. 2005) indicate that the visual $P-L_V$ relation depends on the metal content, but exclude that the metallicity correction follows the linear relation based on the quoted negative empirical γ -value. The nonlinear behavior suggested by the pulsation models accounts quite well for the observed trend.

More recently, Macri et al. (2006, hereinafter [M06]) have presented multiband *BVI* observations of a large Cepheid sample in two fields of the galaxy NGC 4258 with different mean chemical compositions ($\Delta [O/H] \sim 0.5$ dex), and derived a metallicity effect of $\gamma = -0.29$ mag dex $^{-1}$, also excluding any significant variation in the slope of the $P-L$ relations as a function of the Cepheid metal abundance. Their findings agree quite well with the results of a previous investigation by Kennicutt et al. (1998) who found $\gamma = -0.27$ mag dex $^{-1}$ using a sizable sample of Cepheids in two fields of M 101 with a difference in mean oxygen abundance of 0.7 dex.

A vanishing metallicity effect between Galactic and Magellanic Cepheids was also found by Fouque et al. (2007). They collected a sample of 59 calibrating Galactic Cepheids with distances based on robust indicators: HST and Hipparcos trigonometric parallaxes, infrared surface brightness, Interferometric Baade-Wesselink methods and cluster main-sequence fitting. By comparing the slopes of Galactic optical-NIR PL and Wesenheit relations with LMC slopes provided by OGLE (Udalski et al. 1999a) and by Persson et al. (2004) they find no significant difference. Accurate trigonometric parallaxes for ten Galactic Cepheids have been provided by Benedict et al. (2007) using the Fine Guide Sensor available on board the HST. They estimated new optical and NIR PL relations and they found that their slopes are very similar to the slopes of LMC Cepheids.

However, Mottini et al. (2008) analyzed a sizable sample of high-resolution, high signal-

to-noise spectra collected with FEROS@1.5m ESO telescope for Galactic (32) and with UVES@VLT for Magellanic (14 in SMC and 22 in LMC) Cepheids. They found, using individual iron measurements and the same distances adopted by Fouque et al., that the slope of the V –band PL relation does depend on the metal abundance with a confidence level larger than 90%.

In order to overcome current controversy between theory and observations, we undertook a homogeneous analysis of the NGC 4258 Cepheids and a detailed comparison of pulsation predictions with Magellanic Cloud and Galactic Cepheids. In § 2 we present predicted P - L relations, while in § 3 we describe the results of the comparison between theory and observations. The correlation between the Cepheid metallicity and the NGC 4258 oxygen abundance gradient is addressed in § 4 and the conclusions close the paper.

2. Pulsation models

The fiducial P - L relations adopted by M06 are based on unreddened B_0, V_0, I_0 magnitudes of the LMC Cepheids observed by the OGLE II project (Udalski et al. 1999a, hereinafter [U99]) and updated on the OGLE Web site². They are

$$B_0 = 17.368 - 2.439 \log P \quad (1)$$

$$V_0 = 17.066 - 2.779 \log P \quad (2)$$

$$I_0 = 16.594 - 2.979 \log P \quad (3)$$

where P is the pulsation period in days. These relations are used to form intrinsic Period-Color (P - C) relations which are compared with the measured colors to determine the $E(B - V)$, $E(V - I)$, and $E(B - I)$ reddening values for individual Cepheids in NGC 4258. Then, the absolute LMC-relative distance modulus $\delta\mu_0$ of each variable is derived by averaging the three values³

$$\delta\mu_{0,VI} = \delta\mu_I - 1.45E(V - I)$$

$$\delta\mu_{0,BI} = \delta\mu_I - 0.82E(B - I)$$

$$\delta\mu_{0,BVI} = \delta\mu_I - 1.94E(B - V)$$

where $\delta\mu_I$ is the difference between the observed I magnitude and the $I_0(P)$ value from equation (3), while the $A_I/E(B - I)$, $A_I/E(V - I)$, and $A_I/E(B - V)$ ratios are based

²<http://www.astrouw.edu.pl/~ogle>

³The $A_I/E(B - I)=2.38$ value given by M06 is a typo.

on the $A_\lambda/E(B - V)$ values from Table 6 in Schlegel et al. (1998) for $A_V/E(B - V)=3.1$ and the Cardelli et al. (1989) extinction law. However, since equations (1)-(3) were derived by adopting $A_B/E(B - V)=4.32$, $A_V/E(B - V)=3.24$ and $A_I/E(B - V)=1.96$ (see U99), throughout this paper we adopt

$$\delta\mu_{0,VI} = \delta\mu_I - 1.53E(V - I) \quad (4)$$

$$\delta\mu_{0,BI} = \delta\mu_I - 0.83E(B - I) \quad (5)$$

$$\delta\mu_{0,BVI} = \delta\mu_I - 1.96E(B - V), \quad (6)$$

together with

$$\delta\mu_{0,BV} = \delta\mu_V - 3.24E(B - V) \quad (7)$$

where $\delta\mu_V$ is the difference between the observed V magnitude and the $V_0(P)$ value from equation (2).

The quoted approach is equivalent to the classical method of distance determinations based on the reddening free Wesenheit functions. Therefore, we use the computed periods and intensity-averaged M_B, M_V, M_I magnitudes of our fundamental pulsation models with $Z=0.004$ to 0.04 , listed in Table 1, to derive the predicted Period-Wesenheit ($P-W$) relations based on equations (4)-(7), i.e.

$$WVI = M_I - 1.53(M_V - M_I)$$

$$WBI = M_I - 0.83(M_B - M_I)$$

$$WBVI = M_I - 1.96(M_B - M_V)$$

$$WBV = M_V - 3.24(M_V - M_B)$$

In our earlier pulsation models, the adopted luminosity for a given mass and chemical composition was fixed according to Mass-Luminosity (ML) relations based on canonical (“can”) evolutionary computations (Castellani, Chieffi & Straniero 1992; Bono et al. 2000; Girardi et al. 2000). Afterwards, additional models have been computed with higher luminosity levels (“over”) in order to account for a mild convective core overshooting and/or mass loss before or during the Cepheid phase. The overluminous models were constructed by adopting for the chemical compositions representative of Galactic and Magellanic Cepheids the same abundances (helium, metal) and mass values adopted for canonical Cepheid models. This approach allowed us (Bono, Castellani, & Marconi 2000; Caputo et al. 2005) to constrain the impact that the mass-luminosity relation has on pulsation observables. The

quoted assumptions concerning the adopted chemical compositions are supported by theory and observations. Pulsation models constructed by adopting supersolar iron abundance and helium enhanced compositions ($\frac{\Delta Y}{\Delta Z} = 4$) are pulsationally unstable (Fiorentino et al. 2002). Moreover, empirical evidence based on He abundance of Planetary Nebulae suggest a very shallow gradient across the Galactic disk (Stanghellini et al. 2006). Furthermore, chemical evolution models for both the inner and the outer disk indicate similar helium gradients (Hou et al. 2000). Note that current estimates of the helium-to-metal enrichment ratio, $\frac{\Delta Y}{\Delta Z}$, are still affected by large uncertainties. In a recent detailed investigation Casagrande et al. (2007) found, using nearby field K-type dwarf stars, $\frac{\Delta Y}{\Delta Z} = 2.2 \pm 1.1$. The observational scenario is also complicated by the fact that we still lack firm empirical constraints on the linearity of the $\frac{\Delta Y}{\Delta Z}$ relation, when moving from the metal-poor to the metal-rich regime, and on the universality of this relation (Peimbert et al. 2003; Tammann et al. 2008). To account for these uncertainties we constructed sets of Cepheid models by adopting, at fixed metal content, different helium abundances, therefore, the intrinsic error on the zero-point of predicted PL and PW relations include this effect (Fiorentino et al. 2007).

The theoretical Wesenheit functions of each pulsator depend on the adopted luminosity, therefore, to avoid any assumption on the ML relation, we calculated for each model the difference $\log L/L_c$ between the adopted luminosity and the canonical value provided by the Bono et al. (2000) relation

$$\log L_c = 0.90 + 3.35 \log M_e + 1.36 \log Y - 0.34 \log Z \quad (8)$$

where mass and luminosity values are in solar units. Then, by a linear interpolation through all the fundamental models with period $P \sim 4\text{-}80$ days, $Z=0.004\text{-}0.04$, without distinction of the helium content at fixed Z , we derive the linear Period-Wesenheit ($P\text{-}W$) relations listed in Table 2.

According to these predicted $P\text{-}W$ relations, one can determine the true distance modulus μ_0 of individual Cepheids with known metal content, once the $\log L/L_c$ ratio is fixed. In this context, it is worth mentioning that the occurrence either of a mild convective core overshooting during hydrogen burning phases or mass-loss before and/or during the pulsation phases yields positive $\log L/L_c$ values. As a consequence, the $P\text{-}W$ relations for $L=L_c$ provide the *maximum* value of the Cepheid distance. Moreover, we draw attention on the evidence that the metallicity effect on the predicted $P\text{-}W$ relations depends on the adopted Wesenheit function (see also Caputo, Marconi & Musella 2000; F02; F07). In particular, the metallicity dependence of the $P\text{-}WVI$ relation is weak and shows the opposite sign when compared with the other optical $P\text{-}W$ relations. This is warning against the average of the various μ_0 values based on different $P\text{-}W$ relations and, at the same time, provides a plain

method to estimate the Cepheid metal content (see below).

By assuming that the pulsation models listed in Table 1 are actual Cepheids located at the same distance and with the same reddening, but with different chemical abundances, we can derive from equations (1)-(3) their LMC-relative apparent distance moduli μ_B , μ_V and μ_I . Then, by adopting⁴ $\mu_B - \mu_V = E(B - V)$, $\mu_B - \mu_I = E(B - I)$ and $\mu_V - \mu_I = E(V - I)$, we use equations (4)-(7) to determine the four LMC-relative intrinsic values $\delta\mu_{0,VI}$, $\delta\mu_{0,BI}$, $\delta\mu_{0,BVI}$, and $\delta\mu_{0,BV}$.

⁴The comparison of observed colors with the intrinsic P - C relations given by equations (1)-(3) to estimate the reddening values is equivalent to take the differences between two LMC-relative apparent distance moduli and indeed $E(B - V) = (B - V) - (B_0 - V_0) = (B - B_0) - (V - V_0) = \delta\mu_B - \delta\mu_V$.

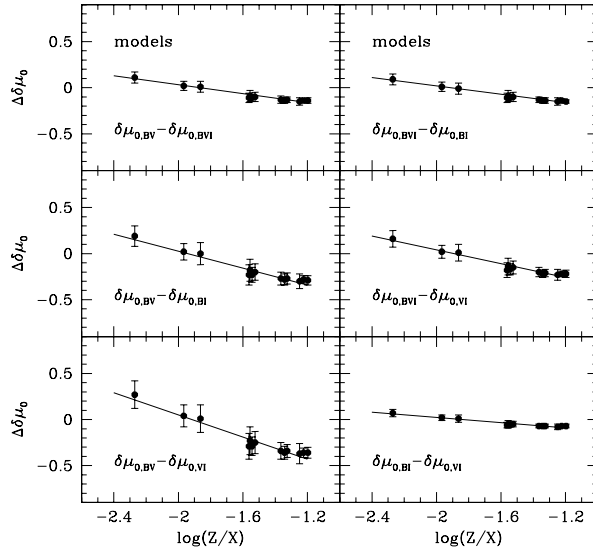


Fig. 1.— Internal differences among LMC-relative distance moduli for fundamental pulsators with $\log P=0.4-1.9$ versus the chemical composition, as listed in Table 4. The lines display the least-squares fit to the data.

By averaging the results over the entire period range ($P \sim 4\text{-}80$ days), without selections between short and long period pulsators, we get the LMC-relative $\delta\mu_0$ values at $L = L_c$ listed in Table 3. As already suggested by the predicted P - W relations given in Table 2, we find that the metallicity effect is *not constant* among the different approaches to estimate the LMC-relative distance moduli. On average, we derive $\gamma(\delta\mu_{0,BV}) \sim -0.59$ mag dex $^{-1}$, $\gamma(\delta\mu_{0,BI}) \sim -0.12$ mag dex $^{-1}$, and $\gamma(\delta\mu_{0,BVI}) \sim -0.35$ mag dex $^{-1}$, whereas the metallicity dependence of $\delta\mu_{0,VI}$ is smaller and seems to depend on the adopted metallicity range. We find $\gamma(\delta\mu_{0,VI}) \sim +0.11$ mag dex $^{-1}$ for $Z \leq 0.02$ and ~ -0.15 for $Z \geq 0.02$, while over the entire metallicity range $Z=0.004\text{-}0.04$, we find $\gamma(\delta\mu_{0,VI}) \sim +0.03$ mag dex $^{-1}$.

In summary, the theoretical results suggest that, if the LMC-based PL_B , PL_V and PL_I relations are used to get the distance to Cepheids with metal content significantly different from the LMC abundance, then the values of the various $\delta\mu_0$ formulations *should not be averaged, but individually considered in order to keep the information provided by their different metal dependence*. Note that if the $\delta\mu_{0,VI}$, $\delta\mu_{0,BI}$, and $\delta\mu_{0,BVI}$ values were averaged to a mean value $\langle\delta\mu_0\rangle$, the ensuing mean metallicity effect would be $\gamma(\langle\delta\mu_0\rangle) \sim -0.15$ mag dex $^{-1}$. This value *cannot* be used to correct distance estimates based on VI magnitudes since it might introduce a systematic error up to ≈ 0.2 mag according to the metallicity range covered by the Cepheids.

A further relevant result of the present study is the predicted metallicity effect on the *internal differences* among the different LMC-relative distance moduli. In particular, these differences revealed to be almost independent of the adopted ML relation. Data plotted in Fig. 1 and listed in Table 4 show that all the differences depend on the pulsator chemical composition. The most metal-sensitive are the $\Delta\delta\mu_{0,BV-VI}$, the $\Delta\delta\mu_{0,BV-BI}$ and the $\Delta\delta\mu_{0,BVI-VI}$. We have already discussed in F07 that these differences provide a robust method to estimate the Cepheid metal content, since they are independent of both distance and reddening.

3. Observed Cepheids

3.1. Magellanic and Galactic variables

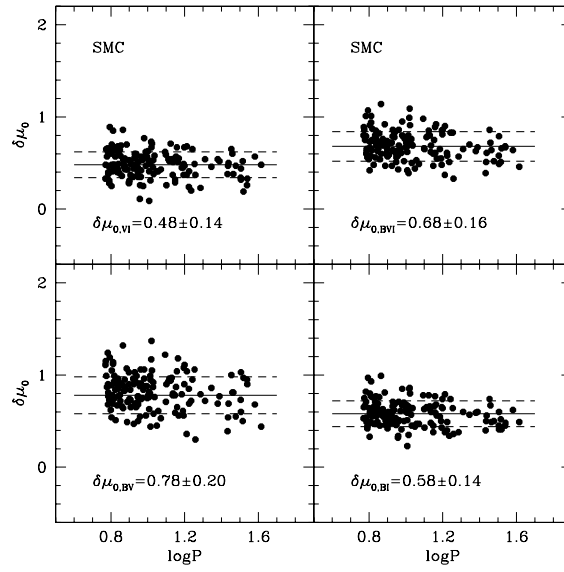


Fig. 2.— LMC-relative distance moduli for OGLE II SMC fundamental Cepheids versus the period. Solid and dashed lines display the average values and the standard deviations, respectively.

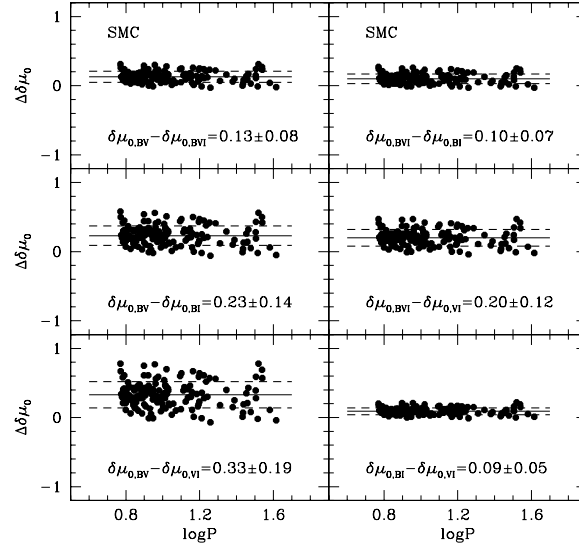


Fig. 3.— Differences among LMC-relative distance moduli for OGLE II SMC fundamental Cepheids versus the period. Solid and dashed lines display the average values and the standard deviations, respectively.

We apply the same procedure described above to the SMC Cepheids collected by the OGLE-II microlensing survey (Udalski et al. 1999b). For the sake of uniformity with the NGC 4258 variables (see later), we use fundamental pulsators with $P \geq 6$ days (~ 200 variables). We derive the mean $\delta\mu_0$ values plotted in Fig. 2 and summarized in Table 5, where the results for the LMC Cepheids (U99) are also given to validate the current approach.

Even though data plotted in Fig. 2 present a large scatter, the four LMC-relative $\delta\mu_0$ formulations do provide different results. In particular, the $\delta\mu_{0,VI}$ gives the shortest LMC-relative distance modulus, in agreement with the theoretical predictions. By using the predicted metallicity effects given in the last row of Table 5 and the Cepheid spectroscopic measurements $[\text{Fe}/\text{H}]_{LMC} = -0.35 \pm 0.15$ dex and $[\text{Fe}/\text{H}]_{SMC} = -0.70 \pm 0.15$ dex (see Luck et al. 1998; Romaniello et al. 2005) and by assuming $\Delta[Z/X]=\Delta[\text{Fe}/\text{H}]$, we find that the measured $\delta\mu_{0,BV}$, $\delta\mu_{0,BI}$, and $\delta\mu_{0,BVI}$ values should be *decreased* by ~ 0.21 , 0.04 and 0.12 mag, whereas the $\delta\mu_{0,VI}$ value should be *increased* by ~ 0.04 mag. Eventually, the discrepancy among the four $\delta\mu_0$ values is mitigated and the metallicity-corrected results yield that the LMC-relative distance modulus of the SMC Cepheids is ~ 0.55 mag, in close agreement with the difference of 0.50 mag determined from eclipsing binaries in the SMC (Hilditch, Howarth & Harries 2005) and in the LMC (Guinan, Ribas & Fitzpatrick 2004).

The differences $\Delta\delta\mu_0$ among the four $\delta\mu_0$ values are summarized in Table 6 and plotted in Fig. 3. The observed variations between SMC and LMC Cepheids agree quite well with pulsation predictions for $\Delta[Z/X]=\Delta[\text{Fe}/\text{H}]=-0.35$, as listed in the last row of Table 6. In addition, the straight comparison between the observed $\Delta\delta\mu_0$ differences and the predicted values listed in Table 4 gives $\log(Z/X)_{LMC} \sim -1.92$ and $\log(Z/X)_{SMC} \sim -2.42$, which are consistent with the spectroscopic iron measurements once we assume $[\text{Fe}/\text{H}]=[Z/X]$ and $(Z/X)_{\odot}=0.024$ (Grevesse et al. 1996). We are aware that the solar chemical composition is under revision and that the recent analysis by Asplund et al. (2004) has decreased the solar chemical abundances by roughly a factor of two, yielding $(Z/X)_{\odot}=0.0165$. However, we adopted the Grevesse et al. (1996) solar abundances, since they are consistent with the model atmospheres (Castelli, Gratton & Kurucz 1997a,b) we use to transform theoretical predictions into the observational plane. The revised abundances are still debated due to the inconsistency with helioseismic results (Bahcall et al. 2005; Guzik et al. 2005). Following the referee’s suggestion, it is also worth noting that evolutionary and pulsation models are constructed by adopting the global metallicity ($[M/H]$) that is a function of both iron and α -element abundances. However, evolutionary prescriptions by Salaris et al. (1993) to estimate the global metallicity were derived using the old solar mixture and we still lack a new relation based on the new solar abundances. Moreover, Salaris & Weiss (1998) found that at solar and super-solar metallicities, the metals affects the evolution. This means that scaled-solar abundances cannot be used to replace the α -enhanced ones of the same total metallicity.

Oxygen is an α -element and intermediate-mass stars with solar abundance typically present solar Oxygen abundances (Gratton et al. 2004). Empirical evidence indicates that field LMC giants present a lower α -enhancement when compared with the Galactic ones (Luck et al. 1998; Hill et al. 2000). However, larger samples are required to constrain the trend in the metal-poor regime (Hill 2004; Venn et al. 2004). It is worth noting that the new solar abundances imply a change in the nebular Oxygen abundance of external galaxies (zero-point and effective temperature of the ionizing stars). To our knowledge we still lack nebular Oxygen abundances in external galaxies accounting for this effect.

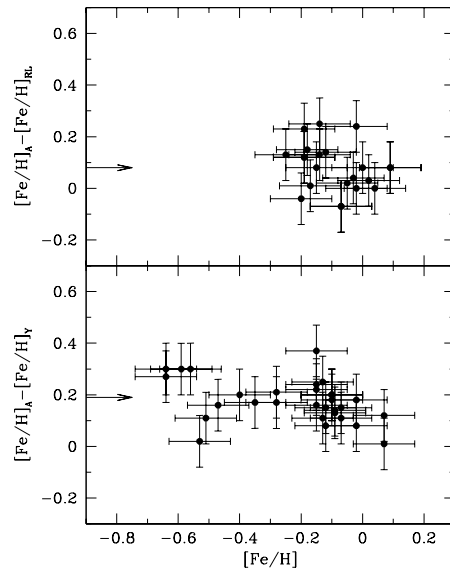


Fig. 4.— Top – Difference in iron abundance $[\text{Fe}/\text{H}]_A - [\text{Fe}/\text{H}]_{RL}$ versus $[\text{Fe}/\text{H}]_{RL}$ for Galactic Cepheids. The arrow shows the adopted average difference. Bottom – Same as the top, but for $[\text{Fe}/\text{H}]_A - [\text{Fe}/\text{H}]_Y$, versus $[\text{Fe}/\text{H}]_Y$.

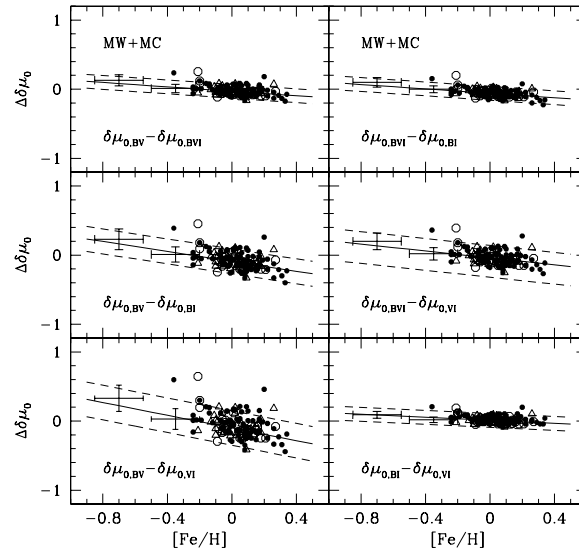


Fig. 5.— Differences among LMC-relative distance moduli for Galactic Cepheids with $P \geq 6$ days versus the three different sets of $[\text{Fe}/\text{H}]$ measurements, $[\text{Fe}/\text{H}]_A$: solid circles, $[\text{Fe}/\text{H}]_Y$: open circles, and $[\text{Fe}/\text{H}]_{RL}$: open triangles in the Andrievsky metallicity scale. The mean values for SMC and LMC variables (crosses) are also plotted. The solid lines are the least square fits to the data, while the dashed lines display the dispersion around the fit. See text for more details.

In order to verify whether this consistency between the pulsation predictions and the Cepheid observed properties also holds up at larger metal abundances, we use the Milky Way variables with measured iron-to-hydrogen ratios. Given the current discrepancy among abundance determinations by different authors, we consider three different sets of measurements: the $[\text{Fe}/\text{H}]_A$ values provided by Andrievsky and collaborators (Andrievsky et al. 2002a,b,c; Andrievsky et al. 2004; Luck et al. 2003; Kovtyukh, Wallerstein & Andrievsky 2005; Luck, Kovtyukh & Andrievsky 2006), the $[\text{Fe}/\text{H}]_{RL}$ values by Romaniello et al. (2005) together with Lemasle et al. (2007), and the $[\text{Fe}/\text{H}]_Y$ values by Yong et al. (2006) together with Fry & Carney (1997). Following Yong et al. (2006) the iron abundances provided by Fry & Carney were decreased by -0.11 dex. The arrows plotted in Fig. 4 show that the $[\text{Fe}/\text{H}]_Y$ and the $[\text{Fe}/\text{H}]_{RL}$ were normalized to the Andrievsky metallicity scale by adding 0.19 and 0.08 dex, respectively.

We also use the BVI magnitudes compiled by Berdnikov, Dambis & Vozyakova (2000). We select the variables with $P \geq 6$ days, although the inclusion of first overtone pulsators has no dramatic effects on the *differences* among the $\delta\mu_0$ values. In fact, adopting $\log P_F = \log P_{FO} + 0.13$, one easily derives that the offsets (first overtone minus fundamental) are ~ -0.08 ($\Delta\delta\mu_{0,BV-VI}$), -0.06 ($\Delta\delta\mu_{0,BV-BI}$), -0.03 ($\Delta\delta\mu_{0,BV-BVI}$), -0.02 ($\Delta\delta\mu_{0,BI-VI}$), -0.05 ($\Delta\delta\mu_{0,BVI-VI}$), and -0.03 mag ($\Delta\delta\mu_{0,BVI-BI}$).

The results plotted in Fig. 5 show that Magellanic and Galactic Cepheids follow reasonably well defined common relations over the metallicity range $[\text{Fe}/\text{H}] = -0.7$ to $+0.3$, with the only exception of CK Pup, HQ Car and TX Cyg (at $[\text{Fe}/\text{H}] = -0.36$, -0.22 and $+0.20$, respectively). Eventually, the linear regression through the Magellanic and Galactic data yields the empirical $\Delta\delta\mu_0$ - $[\text{Fe}/\text{H}]$ calibrations:

$$\Delta\delta\mu_{0,BV-VI} = -0.10(\pm 0.14) - 0.46(\pm 0.08)[Fe/H] \quad \sigma = 0.25 \quad (9)$$

$$\Delta\delta\mu_{0,BV-BI} = -0.09(\pm 0.10) - 0.36(\pm 0.08)[Fe/H] \quad \sigma = 0.18 \quad (10)$$

$$\Delta\delta\mu_{0,BV-BVI} = -0.03(\pm 0.06) - 0.16(\pm 0.03)[Fe/H] \quad \sigma = 0.10 \quad (11)$$

$$\Delta\delta\mu_{0,BI-VI} = +0.01(\pm 0.06) - 0.11(\pm 0.02)[Fe/H] \quad \sigma = 0.10 \quad (12)$$

$$\Delta\delta\mu_{0,BVI-VI} = -0.04(\pm 0.09) - 0.25(\pm 0.05)[Fe/H] \quad \sigma = 0.18 \quad (13)$$

$$\Delta\delta\mu_{0,BVI-BI} = -0.06(\pm 0.05) - 0.16(\pm 0.03)[Fe/H] \quad \sigma = 0.10 \quad (14)$$

where the error in parentheses is the error on the coefficients and the sigma gives the sum in quadrature of the uncertainties affecting both the zero-point and the slope of the fit. These relations are drawn as solid lines in Fig. 5, while the dashed lines display the one σ statistical uncertainty. It is worth emphasizing that the *observed* $\Delta\delta\mu_0$ - $[\text{Fe}/\text{H}]$ relations

based on Magellanic and Galactic Cepheids agree well with the *theoretical* ones presented in Table 4, if we assume $[\text{Fe}/\text{H}]=[\text{Z}/\text{X}]$ and we adopt $(\text{Z}/\text{X})_{\odot}=0.024$ (Grevesse et al. 1996), namely $[\text{Fe}/\text{H}]=\log(\text{Z}/\text{X})+1.62$. Note that an even better agreement is found if we account for the measured overabundance of α -elements for subsolar $[\text{Fe}/\text{H}]$ ratios, as determined by spectroscopic measurements. (see, e.g., Fig. 18 in Yong et al. 2006). This issue will be discussed in a forthcoming paper.

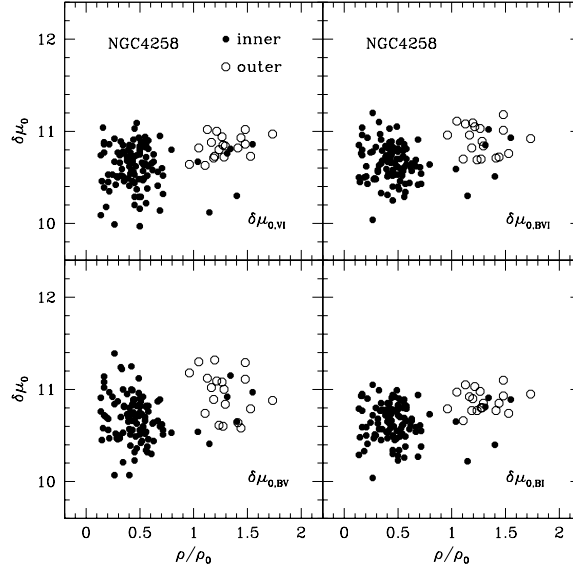


Fig. 6.— LMC-relative distance moduli for NGC 4258 Cepheids with $P \geq 6$ days versus the deprojected radial distance ρ' normalized to $\rho_0=7'.92$. Cepheids located either in the inner or in the outer field are filled and open circles, respectively.

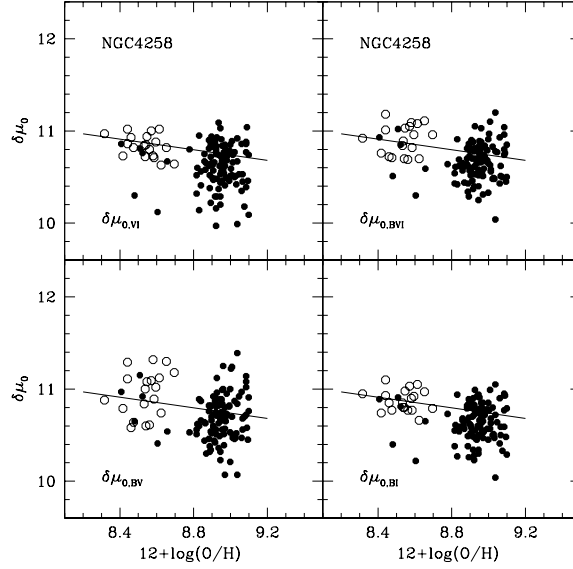


Fig. 7.— Same as in Fig. 6, but with the LMC-relative distance moduli versus the oxygen abundance based on the Za94 gradient. The solid line shows the relation given by M06.

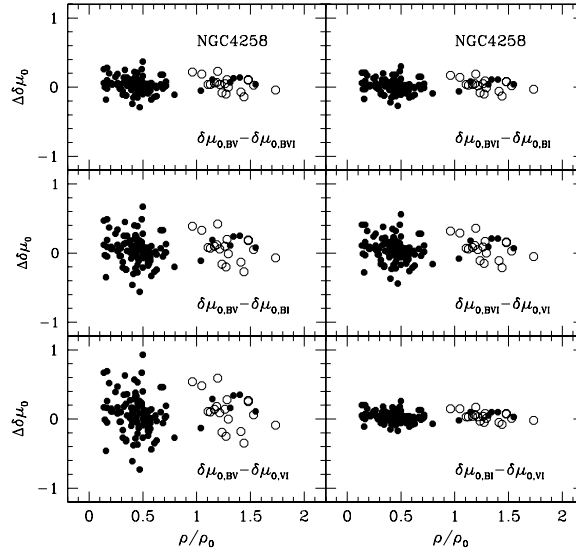


Fig. 8.— Differences among LMC-relative distance moduli for NGC 4258 Cepheids with $P \geq 6$ days versus the deprojected radial distance ρ/ρ_0 . Symbols are the same as in Fig. 6.

3.2. NGC 4258 Cepheids

The Cepheids observed in NGC 4258 belong to two different fields located at different galactocentric distances and whose mean offsets in arcseconds from the nucleus are ≈ -150 (inner field) and $\approx +400$ (outer field) in the East-West direction, while they are $\approx +130$ (inner field) and ≈ -400 (outer field) in the North-South direction.

We apply the same approach already adopted for Magellanic and Galactic variables to the NGC 4258 Cepheids with a variability index $L_V > 2$ (“restricted” sample in M06), $P \geq 6$ days⁵ and errors in the mean BVI magnitudes less than 0.05 mag. The derived LMC-relative distance moduli are plotted in Fig. 6 versus the Cepheid deprojected galactocentric distance $\rho(^{\circ})$ normalized to the isophotal radius $\rho_0=7'.92$, as given⁶ by M06.

Data plotted in Fig. 6 suggest a correlation between the Cepheid distance modulus and its radial distance, with the outer field Cepheids yielding larger distance moduli by about 0.2 mag with respect to those in the inner field. Obviously, such a correlation turns into a chemical abundance dependence of the distance modulus if a metallicity gradient is adopted for the Cepheids. As a fact, using for each individual variable the Za94 relation based on oxygen abundance measurements of H II regions

$$12 + \log(O/H) = 8.97 - 0.49(\rho/\rho_0 - 0.4), \quad (15)$$

where ρ_0 is the isophotal radius equal to $7'.92$, the metallicity effect on the the four LMC-relative distance moduli turns out to be consistent with the M06 value, i.e. $\gamma \sim -0.29 \text{ mag dex}^{-1}$ (see Fig. 7).

⁵The P_{min} adopted by M06 are 6 and 12 days for the Cepheids in the outer and in the inner field, respectively. We adopt the same period cuts for both fields in order to have homogeneous samples.

⁶The ρ/ρ_0 values given by M06 adopt $\rho_0=7'.76$. However, for consistency with the Zaritsky et al. (1994, hereinafter [Z94]) abundance gradient, we normalized them to $\rho_0=7'.92$.

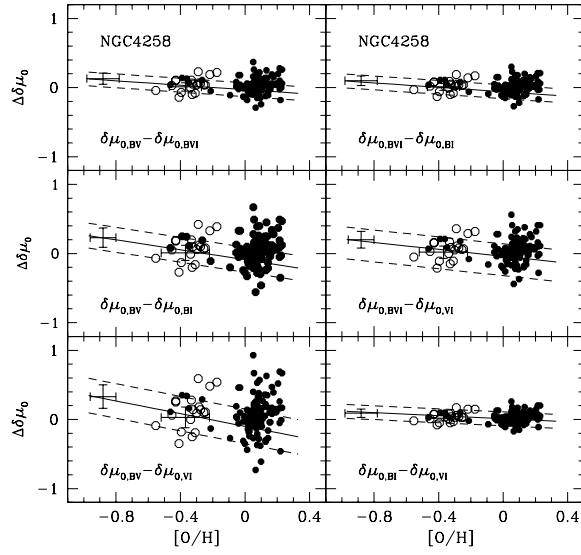


Fig. 9.— Same as in Fig. 8, but with $\Delta\delta\mu_0$ versus the oxygen-to-hydrogen ratio $[O/H]$ based on the galactic gradient given by Za94 and by adopting $\log(O/H)_\odot = -3.13$. The crosses mark the results for SMC and LMC variables. Solid and dashed lines are the same as in Fig. 5, and have been plotted assuming $[Fe/H]=[O/H]$.

However, we show in Fig. 8 that if the individual differences $\Delta\delta\mu_0$ are taken into account, then no clear radial dependence is found, with the Cepheids in both fields yielding quite similar mean $\Delta\delta\mu_0$ values. Data plotted in Fig. 9 show the differences $\Delta\delta\mu_0$ for the NGC 4258 Cepheids versus the oxygen abundance $[\text{O}/\text{H}]_{\text{Za94}} = \log(\text{O}/\text{H})_{\text{NGC4258}} - \log(\text{O}/\text{H})_{\odot}$, following equation (15) and by adopting the solar value $\log(\text{O}/\text{H})_{\odot} = -3.13$ (Grevesse et al. 1996). In order to make an easy comparison, in this figure we also plotted the mean $\Delta\delta\mu_0$ values for SMC and LMC Cepheids (see Table 6) for $[\text{O}/\text{H}] = -0.88 \pm 0.08$ dex and for -0.37 ± 0.15 dex (Ferrarese et al. 2000). The least square fits to the data (solid lines) and their dispersions (dashed lines) showed in Fig. 5 are also plotted in Fig. 9 by assuming that the oxygen abundance is a very robust proxy of the iron abundance (i.e. $[\text{Fe}/\text{H}] = [\text{O}/\text{H}]$). Note that this assumption is fully justified by spectroscopic measurements which yield $[\text{O}/\text{Fe}] = 0 \pm 0.14$ dex over the range $[\text{Fe}/\text{H}] = -0.7$ to $+0.30$ dex (see e.g. Luck et al. 2006). Moreover, recent spectroscopic measurements based on high resolution, high signal-to-noise spectra of 30 Galactic Cepheids (Lemasle et al. 2007) indicate that Oxygen and other α -elements present radial gradients very similar to the iron gradient. This means that Oxygen is a good proxy of the iron content across the Galactic disk. Moreover and even more importantly, empirical evidence indicates that Oxygen nebular abundances agree with absorption line abundances (Hill 2004).

Although the oxygen abundance of the NGC 4258 Cepheids based on the Za94 oxygen abundance gradient, is within the range spanned by Magellanic and Milky Way Cepheids, the observed $\Delta\delta\mu_0$ values of several variables in the inner field deviate from the “empirical” $\Delta\delta\mu_0$ - $[\text{O}/\text{H}]$ relations provided by Magellanic and Galactic variables. This evidence indicates that Cepheids in NGC 4258 might have a metal content that is significantly lower than the oxygen abundance based on their radial distance.

To make clear this feature, we select the inner field Cepheids with $\rho/\rho_0 < 0.7$ (sample A) and the outer field Cepheids with $\rho/\rho_0 > 1.0$ (sample B) for which the mean oxygen abundance suggested by the Za94 gradient is $[\text{O}/\text{H}]_{\text{Za94}} = +0.13 \pm 0.08$ and -0.37 ± 0.09 dex, respectively. We show in Table 7 and Table 8 that the two samples have different LMC-relative distance moduli but nearly identical mean $\Delta\delta\mu_0$ values, at odds with the behavior of Magellanic and metal-rich Milky Way variables, as listed in the same Table 8. In conclusion, the observed $\Delta\delta\mu_0$ values would suggest an average LMC-like oxygen abundance $[\text{O}/\text{H}] \sim -0.4$ dex for all the NGC 4258 Cepheids. This result agrees with the Za94-based mean value of the outer field, whereas for the inner field the oxygen content provided by the radial distance appears to be 1.3 times larger than the solar value.

We do not found any reason to distrust this intriguing result, since the selection criteria adopted by M06 are very robust, and indeed, we only use objects with errors in mean B, V, I

magnitudes smaller than 0.05 mag. The adopted $P_{min}=6$ days should avoid contamination by first overtone Cepheids, although the effects of period uncertainties on the $\Delta\delta\mu_0$ differences are quite small and first overtone pulsators should give smaller $\Delta\delta\mu_0$ values than fundamental pulsators with the same period. However the selection of Cepheids with $P \leq 10$ days is more difficult, in particular in the inner field (see M06). Therefore, we performed a new test by removing these short period variables from the sample and we found that the new results are almost identical to those listed in Table 7 and Table 8.

Eventually, it seems plausible to suspect that either the Za94 oxygen gradient requires a revision, or the galactic location cannot be used as a reliable metallicity parameter for individual Cepheids, or a combination of the above effects.

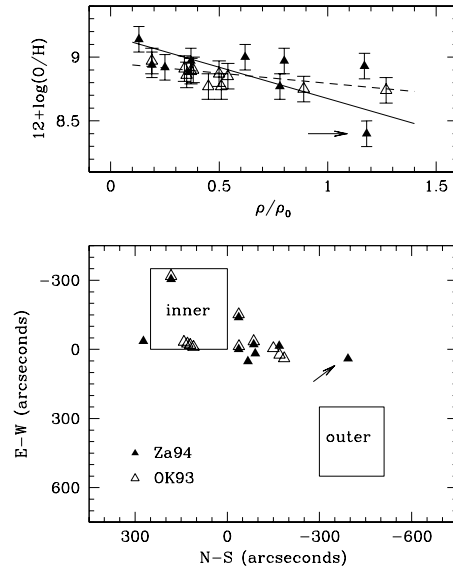


Fig. 10.— Top – Nebular oxygen abundances measured by Za94 (filled triangles) and by OK93 (open triangles) versus the fractional isophotal radius with $\rho_0=7'.92$. The solid line shows the Za94 relation, while the dashed line is based on equation (16), and it was estimated by neglecting the H II region marked by the arrow. Bottom – Positions of the H II regions observed by Za94 and by OK93 in comparison with the NGC 4258 inner and outer fields.

4. Cepheid metal content and galactic abundance gradient

In the top panel of Fig. 10, we plot Za94 and previous oxygen abundance measurements by Oey & Kennicutt (1993, hereinafter [OK93]) versus the fractional isophotal radius with $\rho_0=7'.92$. It is quite clear that the variations in abundance among external regions with $\rho/\rho_0 \sim 1.2$ are greater than the abundance uncertainties and that the lowest value ($12+\log(\text{O}/\text{H})=8.4$) measured by Za94 at $\rho/\rho_0=1.18$ strongly affects the slope of equation (15). Indeed, if we neglect this value the linear fit to all the Za94 and the OK93 measurements yields (dashed line) a significantly flatter gradient, namely

$$12 + \log(\text{O}/\text{H}) = 8.89 - 0.16(\rho/\rho_0 - 0.4) \quad (16)$$

The bottom panel of Fig. 10 shows that all the Cepheids in the NGC 4258 inner field are located close to H II regions where, as described by equation (16), the oxygen abundance has the almost constant solar value, i.e. $12+\log(\text{O}/\text{H})=8.86\pm 0.08$. On the other hand, the variables in the outer field are distant from any observed H II region, and only marginally close to the H II region underabundant in oxygen ($12+\log(\text{O}/\text{H})=8.4$). Even though, we assume a tight star-by-star correlation between oxygen abundance and radial distance, we find that by using the equation (16) to estimate the individual abundances of NGC 4258 Cepheids would yield a mean abundance difference of only ~ 0.15 dex between the inner and the outer field. This would imply that the NGC 4258 is not the right laboratory to constrain the metallicity effect on the LMC-relative distance moduli. On the other hand, the assumption of a lower oxygen abundance for the outer field variables would imply that the galactic gradient becomes significantly steeper when moving from the western to the eastern direction.

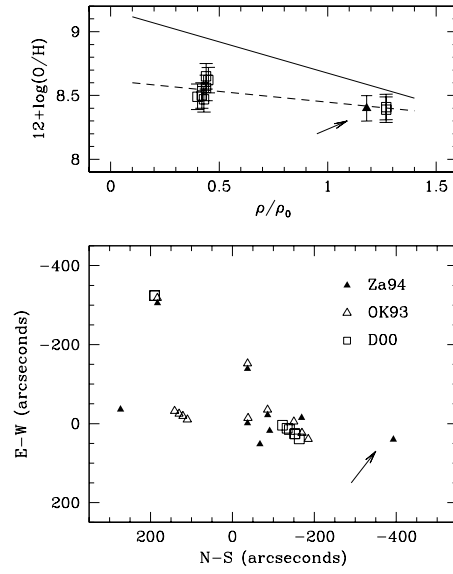


Fig. 11.— Top — Nebular oxygen abundances measured by D00 versus the fractional isophotal radius with $\rho_0=7'.92$. The solid line is the Za94 oxygen gradient, while the dashed line is the best fit line given by equation (17). Bottom — Positions of the H II regions observed by Za94, by OK93 and by D00.

Although the occurrence of spatial asymmetric metallicity gradients cannot be ruled out (see, e.g., Kennicutt & Garnett 1996), we draw the attention on recent observations specifically addressed to study extragalactic H II regions which were expected to be metal-rich. As a whole, the new measurements (see, e.g., Kennicutt, Bresolin & Garnett 2003; Bresolin, Garnett & Kennicutt 2004; Bresolin et al. 2005) yield a significant decrease in the nebular oxygen abundances of regions more metal-rich than LMC, and marginally affect the abundances of metal-poor ones. Therefore, the galactic gradients become significantly shallower than those estimated by previous determinations.

In this context it is worth mentioning that Diaz et al. (2000, hereinafter [D00]), by performing a more detailed analysis of optical and near-infrared observations of several NGC 4258 regions previously observed by Za94 and by OK93, measured oxygen abundances that are on average a factor of two lower. Data plotted in Fig. 11 disclose that, by using the new and more accurate D00 abundances, the NGC 4258 abundance gradient can be (dashed line)

$$12 + \log(O/H) = 8.55 - 0.17(\rho/\rho_0 - 0.4), \quad (17)$$

which implies a LMC-like mean oxygen abundance for both the inner (sample A: $[O/H] = -0.32 \pm 0.08$) and the outer field Cepheids (sample B: $[O/H] = -0.49 \pm 0.09$). This would also imply a reasonable agreement with the predicted correlation between the metal abundance and the $\Delta\delta\mu_0$ values.

5. Conclusions and final remarks

In the above sections, we have shown that both the comparison with pulsation models and the most recent H II abundance measurements suggest a rather constant, LMC-like metal content for the Cepheids observed in the two fields of NGC 4258. This finding, once confirmed, would prevent any reliable differential determination of the P - L metallicity dependence. As a consequence, the observed difference of ~ 0.20 mag in distance modulus between outer and inner field variables might be caused by other observational effects rather than a difference in metal abundance.

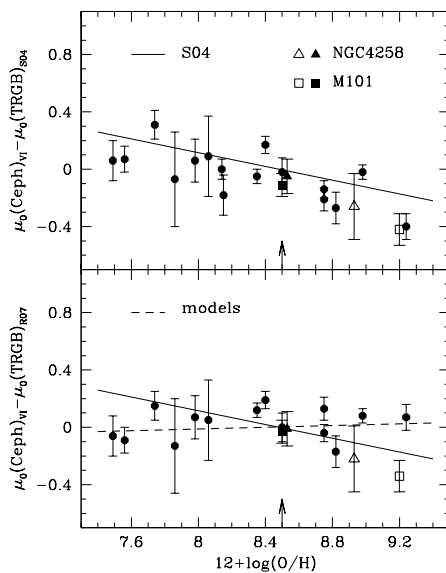


Fig. 12.— Top – Difference between Cepheid (VI -based) and TRGB distances from Sakai et al. (2004, [S04]), as a function of the nebular oxygen abundance in the Za94 scale. The arrow marks the LMC, while filled and open symbols display the outer and the inner fields in M 101 and in NGC 4258, respectively. The solid line was drawn using the S04 value $\gamma = -0.25 \text{ mag dex}^{-1}$. Bottom – Same as the top, but with the TRGB distances according to Rizzi et al. (2007, [R07]). The dashed line was drawn using the value $\gamma = +0.05 \text{ mag dex}^{-1}$ of the predicted P - WVI relation.

We are facing the evidence that the NGC 4258 results presented by M06 agree quite well with the metallicity effect $\gamma = -0.24 \text{ mag dex}^{-1}$ determined by Kennicutt et al. (1998) from Cepheid observations in two fields of M 101. However, it is worthy mentioning that Macri et al. (2001) brought forward the hypothesis that blended Cepheids could be responsible for a large fraction of the difference in distance modulus between the outer and the inner field in M 101. We recall that blended Cepheids, which are mainly expected in the crowded inner galactic fields, appear brighter than they really are and that their distances are systematically underestimated by $\sim 6\text{-}9\%$ (see Mochejska et al. 2000), leading to μ_0 underestimated by approximately 0.1-0.2 mag.

Moreover, the $\gamma = -0.25 \text{ mag dex}^{-1}$ provided by Sakai et al. (2004, hereinafter [S04]) from the comparison of distances based on Cepheid variables and on the tip of the red giant branch (TRGB) has been recently questioned by Rizzi et al. (2007, hereinafter [R07]). By adopting the distance determinations listed in Table 9, we plot in the top panel of Fig. 12 the S04 difference between the Cepheid, based on the LMC $P-L_V$ and $P-L_I$ relations, and the TRGB distances versus the Za94 nebular oxygen abundances. The data⁷ clearly indicate a trend with metallicity, with the Cepheid residual distance modulus decreasing with increasing oxygen abundance and leading to $\gamma = -0.25 \text{ mag dex}^{-1}$ (solid line). However, data plotted in the bottom panel of this figure show that distance determinations provided by R07 using the TRGB method agree within the errors, with Cepheid distances, *with the exception of M 101 and NGC 4258 inner fields*, over the entire metallicity range. Note that in this case we neglected the metallicity correction. The agreement becomes even better if we adopt the $\gamma=+0.05 \text{ mag dex}^{-1}$ value of the predicted $P\text{-}WVI$ relation (dashed line).

⁷Cepheid and TRGB distance scales are normalized to $\mu_0(\text{LMC})=18.50 \text{ mag}$. To the S04 original distances we added the current Cepheid distances to NGC 4258 and to SMC, and the WLM Cepheid distance by Pietrzynski et al. (2007).

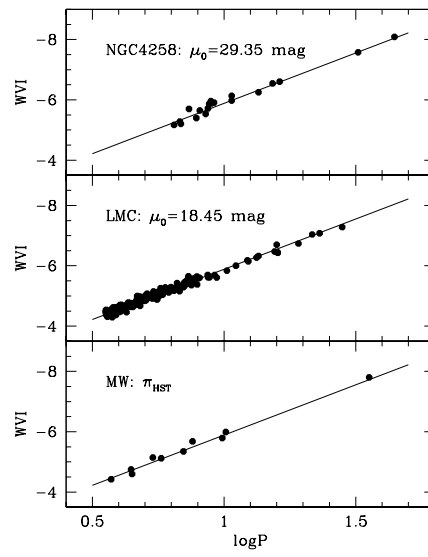


Fig. 13.— Bottom — Absolute P - WVI relation for Galactic Cepheids with HST trigonometric parallaxes. This relation is used to derive the true distance modulus of Cepheids in the LMC (middle) and in the outer field of NGC 4258 (top), by neglecting the metallicity correction.

As a final test of the metallicity effect on Cepheid distances based on VI magnitudes we adopted the Galactic Cepheids with *HST* trigonometric parallaxes (Benedict et al. 2007). From the absolute WVI functions of these variables, we find that they obey to the P - WVI relation $WVI = -2.55 - 3.33 \log P$, as shown by the solid line in the bottom panel of Fig. 13. By using this relation for the Cepheids in the LMC and in the outer field of NGC 4258 *by neglecting the metallicity correction*, we derive $\mu_{0,VI}(\text{LMC}) = 18.45 \pm 0.09$ mag and $\mu_{0,VI}(\text{NGC4258}) = 29.35 \pm 0.12$ mag, which are both only slightly *larger* than $\mu_0(\text{LMC}) = 18.41 \pm 0.09$ mag determined by Guinan, Ribas & Fitzpatrick (2004) from eclipsing binaries (EB) and $\mu_0(\text{NGC4258}) = 29.29 \pm 0.15$ mag based on the maser geometric distance measured by Herrstein et al. (1999). But, the variables in the LMC and in the outer field of NGC 4258 *do* have a lower metal abundance by ~ -0.4 dex than the Galactic variables and the adoption of the M06 value $\gamma = -0.29$ mag dex $^{-1}$ would *increase* the distance moduli to $\mu_{0,VI}(\text{LMC}) = 18.56 \pm 0.09$ mag and $\mu_{0,VI}(\text{NGC4258}) = 29.46 \pm 0.12$ mag, causing metallicity corrected Cepheid distances which are larger by about 0.15-0.17 mag than EB and maser distance determinations. It goes without saying that by adopting $\gamma = +0.05$ mag dex $^{-1}$ from the predicted P - WVI relation would further improve the consistency between the Cepheid distances and the quoted EB and maser-based determinations.

In summary, the main findings of the current paper are the following:

the theoretical pulsation models suggest that both the sign and the amount of the metallicity dependence of the P - W relations depend on the chosen passbands. In particular, for distances based on BVI magnitudes, the predicted metallicity effect on μ_0 varies from $\gamma \sim -0.61$ mag dex $^{-1}$ (P - WBV relation) to $\gamma \sim +0.05$ mag dex $^{-1}$ (P - WVI relation) over the range $Z = 0.004$ - 0.04 . These predictions are supported by the comparison of SMC and Milky Way Cepheids with LMC variables.

Accurate BVI photometry of Cepheids in two fields of NGC 4258 leads to a systematic difference in the true distance moduli of $\sim +0.2$ mag between the outer and the inner field. Adopting for individual Cepheids the oxygen abundance given by their galactocentric distance and the abundance gradient of Z94, one derives a metallicity effect $\gamma \sim -0.29$ mag dex $^{-1}$ which is consistent with an earlier $\gamma \sim -0.24$ mag dex $^{-1}$ found by Kennicutt et al. (1998) from Cepheids in two fields of M 101.

The comparison with pulsation models as well as with Magellanic and Galactic variables, indicates a rather small abundance difference between the NGC 4258 inner and outer fields, in agreement with recent nebular oxygen abundances by Diaz et al. (2000).

As a whole, the two “direct” determinations of the metallicity effect which provide negative metallicity dependence $\gamma \sim -0.24$ and -0.29 mag dex $^{-1}$ appear undermined by the

lack of a significant difference in metal abundance (NGC 4258) or by the possible occurrence of blended Cepheids in the inner field (M 101).

The comparison of VI -based Cepheid distances with independent determinations based on the TRGB (external galaxies), *HST* trigonometric parallaxes (Milky Way Cepheids), eclipsing binaries (Large Magellanic Cloud) and water maser (NGC 4258) does not support the negative empirical γ values. Current results seem to favor the predicted value $\gamma \sim +0.05 \text{ mag dex}^{-1}$.

It is a pleasure to thank A. Diaz and L. Rizzi for useful discussions on nebular abundance measurements and on distance determinations to external galaxies based on the TRGB method. We also thank N. Patat for several insights on the projected distances, F. Thevenin and A. Walker for a detailed reading of an early draft of this paper. We acknowledge an anonymous referee for his/her suggestions that improved the content and the readability of the manuscript.

REFERENCES

- Asplund, M., Grevesse, N., Sauval, A. J., Allende Prieto, C., Kiselman, D. 2004, *A&A*, 417, 751
- Andrievsky, S. M., Kovtyukh, V. V., Luck, R. E. 2002a, *A&A*, 381, 32
- Andrievsky, S. M., Bersier, D., Kovtyukh, V. V. 2002b, *A&A*, 384, 140
- Andrievsky, S. M., Kovtyukh, V. V., Luck, R. E. 2002c, *A&A*, 392, 491
- Andrievsky, S. M., Luck, R. E., Martin, P., Lapine, J. R. D. 2004, *A&A*, 413, 159
- Bahcall, J. N., Serenelli, A. M., Basu, S., 2005, *ApJ*, 621, 85
- Benedict, G. F., et al. 2007, *AJ*, 133, 181
- Berdnikov, L. N., Dambis, A. K., Vozyakova, O. V. 2000, *A&AS*, 143, 211
- Bono, G., Caputo, F., Cassisi, S., et al. 2000, *ApJ*, 543, 955
- Bresolin, F.; Garnett, D. R.; Kennicutt, R. C., Jr., 2004, *ApJ*, 615, 228
- Bresolin, F., Schaerer, D., Gonzalez Delgado, R. M., Stasin'ska, G., 2005, *A&A*, 441, 981
- Caputo, F. 2008, *Mem. Sait*, in press

- Caputo, F., Marconi, M., Musella, I. 2000, *A&A*, 354, 610
- Caputo, F.; Bono, G.; Fiorentino, G.; Marconi, M.; Musella, I., 2005, *ApJ*, 629, 1021
- Cardelli, J. A., Clayton, G. C., Mathis, J. S., 1989, *ApJ*, 345, 245
- Casagrande, L.; Flynn, C., Portinari, L.; Girardi, L.; Jimenez, R. 2007, *MNRAS*, 382, 1516
- Castellani, V., Chieffi, A., & Straniero, O. 1992, *ApJS*, 78, 517
- Castelli, F., Gratton, R. G., & Kurucz, R. L. 1997a, *A&A*, 318, 841
- Castelli, F., Gratton, R. G., & Kurucz, R. L. 1997b, *A&A*, 324, 432
- Díaz, A. I., Castellanos, M., Terlevich, E., Luisa García-Vargas, M. 2000, *MNRAS*, 318, 462 [D00]
- Ferrarese, L., et al. 2000, *ApJS*, 128, 431
- Fiorentino, G., Caputo, F., Marconi, M., Musella, I. 2002, *ApJ*, 576, 402 [F02]
- Fiorentino, G., Marconi, M., Musella, I., Caputo, F. 2007, *A&A*, 476, 863 [F07]
- Fouqué, P., et al. 2007, *A&A*, 476, 73
- Freedman, W. L., Hughes, S. M., Madore, B. F., et al. 1994, *ApJ*, 427, 628
- Fry, A. M., & Carney, B. W. 1997, *AJ*, 113, 1073
- Girardi, L., Bressan, A., Bertelli, G., Chiosi, C. 2000, *A&AS*, 141, 371
- Gratton, R., Sneden, C., & Carretta, E. 2004, *ARA&A*, 42, 385
- Grevesse, N., Noels, A., & Sauval, A. J., 1996, *ASPC*, 99, 117
- Groenewegen, M. A. T., Romaniello, M., Primas, F., Mottini, M. 2004, *A&A*, 420, 655
- Guinan, E. F., Ribas, I., Fitzpatrick, E. L. 2004, in *Variable Stars in the Local Group*, IAU Coll. 193, ed. D. W. Kurtz and K. R. Pollard (San Francisco, ASP), 363
- Guzik, J. A., Watson, L. S., Cox, A. N., 2005, *ApJ*, 627, 1049
- Herrnstein, J. R., et al. 1999, *Natur*, 400, 539
- Hilditch, R. W., Howarth, I. D., Harries, T. J., 2005, *MNRAS*, 357, 304
- Hill, V., Francois, P., Spite, M., Primas, F., Spite, F. 2000, *A&A*, 364, L19

- Hill, V. 2004, in *Origin and Evolution of the Elements* ed. A. McWilliam and M. Rauch (Cambridge: Cambridge Univ. press), 203
- Hou, J. L., Prantzos, N., Boissier, S. 2000, *A&A*, 362, 921
- Kanbur, S. M., Ngeow, C., Nikolaev, S., Tanvir, N. R., Hendry, M. A. 2003, *A&A*, 411, 361
- Kennicutt, R. C., Jr., Bresolin, F., Garnett, D. R. 2003, *PASP*, 115, 928
- Kennicutt, R. C., Jr., Garnett, D. R. 1996, *ApJ*, 456, 504
- Kennicutt, R. C., Jr., Stetson, P. B., Saha, A. 1998, *ApJ*, 498, 181
- Kovtyukh, V. V., Wallerstein, G., Andrievsky, S. M., 2005, *PASP*, 117, 1173
- Lemasle, B., Francois, P., Bono, G., Mottini, M., Primas, F., Romaniello, M. 2007, *A&A*, 467, 283
- Luck, R. E., Gieren, W. P., Andrievsky, S. M., Kovtyukh, V. V., Fouque, P., P ont, F., Kienzle, F. 2003, *A&A*, 401, 939
- Luck, R. E., Kovtyukh, V. V., Andrievsky, S. M. 2006, *AJ*, 132, 902
- Luck, R. E., Moffett, T. J.; Barnes, T. G. III, Gieren, W. P. 1998, *AJ*, 115, 605
- Macri, L. M., Stanek, K. Z., Bersier, D., Greenhill, L. J., Reid, M. J. 2006, *ApJ*, 652, 1133 [M06]
- Macri, L. M. et al. 2001, *ApJ*, 549, 721
- Marconi, M., Musella, I., Fiorentino, G., 2005, *ApJ*, 632, 590 [M05]
- Mochejska, B. J., Macri, L. M., Sasselov, D. D., Stanek, K. Z. 2000, *AJ*, 120, 810
- Mottini, M., et al. 2008, *A&A*, accepted
- Ngeow, C.-C., & Kanbur, S.M. 2004, *MNRAS*, 349, 1130
- Oey, M. S., Kennicutt, R. C. Jr. 1993, *ApJ*, 411, 137 [OK93]
- Peimbert, M.; Peimbert, A.; Luridiana, V.; Ruiz, M. T. 2003, in *Star Formation Through Time*, ed. E. Perez, R. M. Gonzalez Delgado, G. Tenorio-Tagle (San Francisco, ASP), 81
- Persson, S. E., Madore, B. F., Krzeminski, W., Freedman, W. L., Roth, M., Murphy, D. C. 2004, *AJ*, 128, 2239

- Pietrzynski, G., et al. 2007, *AJ*, 134, 594
- Rizzi, L., Tully, R. B., Makarov, D., Makarova, L., Dolphin, A. E., Sakai, S., Shaya, E. J. 2007, *ApJ*, 661, 815 [R07]
- Romaniello, M., Primas, F., Mottini, et al. 2005, *A&A*, 429, 37
- Saha, A., Labhardt, L., Schwengeler, H., Macchetto, F. D., Panagia, N., Sandage, A., & Tammann, G. A. 1994, *ApJ*, 425, 14
- Sakai, S., Ferrarese, L., Kennicutt, R. C., Jr., Saha, A. 2004, *ApJ*, 608, 42 [S04]
- Salaris, M., Chieffi, A., & Straniero, O. 1993, *ApJ*, 414, 580
- Salaris, M.; & Weiss, A. 1998, *A&A*, 335, 943
- Sandage, A., Tammann, G. A., & Reindl, B. 2004, *A&A*, 424, 43
- Sasselov, D.D., Beaulieu, J. P., Renault, C. 1997, *A&A*, 324, 471
- Schlegel, D. J., Finkbeiner, D. P., Davis, M., 1998, *ApJ*, 500, 525
- Stanghellini, L., Guerrero, M.-A., Cunha, Ka., Manchado, A., Villaver, E. 2006, *ApJ*, 651, 898
- Storm, J., Carney, B. W., Gieren, W. P., Fouqu, P., Latham, D. W., Fry, A. M. 2004, *A&A*, 415, 531
- Tammann, G.A., Sandage, A., Reindl, B. 2003, *A&A*, 404, 423
- Tammann, G.A., Sandage, A., Reindl, B. 2008, *ApJ*, accepted, arXiv:0712.2346
- Udalski, A., Soszynski, I., Szymanski, M. et al. 1999a, *AcA*, 49, 223 [U99]
- Udalski, A., Soszynski, I., Szymanski, M., Kubiak, M., Pietrzynski, G., Wozniak, P., Zebrun, K. 1999b, *AcA*, 49, 437
- Venn, K. A., Irwin, M., Shetrone, M. D., Tout, C. A., Hill, V., Tolstoy, E. 2004, *AJ*, 128, 1177
- Yong, D., Carney, B. W., Teixeira de Almeida, M. L., Pohl, B. L. 2006, *AJ*, 131, 2256
- Zaritsky, D., Kennicutt, R. C., Jr., Huchra, J. 1994, *ApJ*, 420, 87 [Z94]

Table 1. Basic parameters of fundamental pulsation models. The adopted luminosity refers to Mass-Luminosity relations based on canonical (“can”) evolutionary computations or deals with higher luminosity levels (“over”) produced by mild convective core overshooting and/or mass loss before or during the Cepheid phase.

Z	Y	M/M_{\odot}	$\log L/L_{\odot}$
(1)	(2)	(3)	(4)
0.004	0.25	3.5-11.0	can, over
0.008	0.25	3.5-11.0	can, over
0.01	0.26	5.0-11.0	can
0.02	0.25, 0.26, 0.28, 0.31	5.0-11.0	can, over
0.03	0.275, 0.31, 0.335	5.0-11.0	can
0.04	0.25, 0.29, 0.33	5.0-11.0	can

Table 2. Predicted P - W relations for fundamental pulsators with $Z=0.004$ - 0.04 and based on intensity-averaged magnitudes.

W	α	β	γ	δ
(1)	(2)	(3)	(4)	(5)
$W = \alpha + \beta \log P + \gamma \log(Z/X) + \delta \log(L/L_c)$				
WBV	-3.90 ± 0.09	-3.79 ± 0.03	-0.61 ± 0.03	$+0.64 \pm 0.04$
WVI	-2.82 ± 0.13	-3.24 ± 0.05	$+0.05 \pm 0.03$	$+0.81 \pm 0.04$
WBI	-3.05 ± 0.09	-3.36 ± 0.02	-0.11 ± 0.03	$+0.76 \pm 0.04$
$WBVI$	-3.47 ± 0.06	-3.57 ± 0.02	-0.35 ± 0.03	$+0.70 \pm 0.04$

Table 3. Average LMC-relative absolute distance moduli of canonical ($L=L_c$) fundamental pulsation models with the labeled metal (Z) and helium (Y) content.

Z	Y	$\log(Z/X)$	$\delta\mu_{0,BV}$	$\delta\mu_{0,VI}$	$\delta\mu_{0,BI}$	$\delta\mu_{0,BVI}$
(1)	(2)	(3)	(4)	(5)	(6)	(7)
0.004	0.250	-2.271	-18.46±0.06	-18.75±0.12	-18.66±0.09	-18.57±0.05
0.008	0.250	-1.967	-18.72±0.05	-18.77±0.10	-18.75±0.08	-18.74±0.05
0.010	0.260	-1.863	-18.72±0.07	-18.73±0.12	-18.72±0.09	-18.72±0.06
0.020	0.250	-1.562	-18.99±0.08	-18.70±0.10	-18.76±0.09	-18.88±0.06
0.020	0.260	-1.556	-18.97±0.07	-18.74±0.11	-18.79±0.09	-18.88±0.05
0.020	0.280	-1.544	-18.94±0.08	-18.67±0.12	-18.73±0.11	-18.84±0.09
0.020	0.310	-1.525	-18.90±0.04	-18.65±0.11	-18.70±0.09	-18.80±0.05
0.030	0.275	-1.365	-19.05±0.07	-18.72±0.09	-18.79±0.08	-18.92±0.06
0.030	0.310	-1.342	-19.00±0.07	-18.64±0.09	-18.71±0.09	-18.86±0.07
0.030	0.335	-1.326	-18.98±0.07	-18.64±0.08	-18.71±0.08	-18.85±0.07
0.040	0.250	-1.249	-19.20±0.08	-18.82±0.07	-18.90±0.06	-19.05±0.06
0.040	0.290	-1.224	-19.13±0.06	-18.77±0.06	-18.84±0.07	-18.99±0.06
0.040	0.330	-1.197	-19.07±0.08	-18.71±0.06	-18.78±0.06	-18.93±0.07

Table 4. Internal differences among the LMC-relative absolute distance moduli listed in Table 1 for fundamental pulsators with the labeled metal (Z) to hydrogen (X) ratio and $\log P=0.4-1.9$. The coefficients of the linear least-squares fits to the data are given in the last two lines.

$\log(Z/X)$	$\Delta\delta\mu_{0,BV-VI}$	$\Delta\delta\mu_{0,BV-BI}$	$\Delta\delta\mu_{0,BV-BVI}$	$\Delta\delta\mu_{0,BI-VI}$	$\Delta\delta\mu_{0,BVI-VI}$	$\Delta\delta\mu_{0,BVI-BI}$
(1)	(2)	(3)	(4)	(5)	(6)	(7)
-2.27	+0.27±0.14	+0.19±0.11	+0.11±0.06	+0.07±0.05	+0.16±0.08	+0.09±0.06
-1.97	+0.04±0.11	+0.02±0.09	+0.02±0.05	+0.02±0.04	+0.02±0.08	+0.01±0.05
-1.86	+0.01±0.14	+0.00±0.12	+0.01±0.06	+0.01±0.05	+0.01±0.09	-0.01±0.06
-1.56	-0.29±0.13	-0.23±0.11	-0.11±0.05	-0.06±0.05	-0.18±0.09	-0.11±0.05
-1.55	-0.23±0.15	-0.18±0.12	-0.09±0.06	-0.05±0.05	-0.14±0.09	-0.09±0.06
-1.54	-0.29±0.10	-0.23±0.08	-0.11±0.04	-0.06±0.03	-0.17±0.06	-0.11±0.04
-1.53	-0.25±0.11	-0.20±0.09	-0.10±0.05	-0.05±0.05	-0.15±0.07	-0.10±0.05
-1.36	-0.34±0.08	-0.27±0.07	-0.13±0.04	-0.07±0.04	-0.20±0.06	-0.13±0.03
-1.34	-0.36±0.07	-0.28±0.06	-0.14±0.03	-0.07±0.03	-0.22±0.05	-0.14±0.03
-1.33	-0.34±0.06	-0.27±0.06	-0.13±0.03	-0.07±0.03	-0.21±0.05	-0.14±0.03
-1.25	-0.37±0.10	-0.30±0.08	-0.15±0.04	-0.08±0.03	-0.23±0.06	-0.15±0.04
-1.22	-0.36±0.05	-0.28±0.04	-0.14±0.03	-0.07±0.02	-0.22±0.03	-0.14±0.03
-1.20	-0.36±0.06	-0.29±0.05	-0.14±0.03	-0.07±0.03	-0.22±0.04	-0.15±0.02
	$\Delta\delta\mu_0=A+B\log(Z/X)$					
A	-1.15±0.05	-0.89±0.04	-0.45±0.02	-0.26±0.02	-0.70±0.03	-0.44±0.02
B	-0.60±0.05	-0.46±0.04	-0.24±0.02	-0.14±0.02	-0.37±0.03	-0.23±0.02

Table 5. Average LMC-relative absolute distance moduli for LMC and SMC fundamental Cepheids with $P \geq 6$ days. The last line gives the corrected values for SMC variables according to the predicted metallicity effects: $\gamma(\delta\mu_{0,BV}) \sim -0.59 \text{ mag dex}^{-1}$, $\gamma(\delta\mu_{0,VI}) \sim +0.11 \text{ mag dex}^{-1}$, $\gamma(\delta\mu_{0,BI}) \sim -0.12 \text{ mag dex}^{-1}$, and $\gamma(\delta\mu_{0,BVI}) \sim -0.35 \text{ mag dex}^{-1}$

Galaxy	[Fe/H]	$\delta\mu_{0,BV}$	$\delta\mu_{0,VI}$	$\delta\mu_{0,BI}$	$\delta\mu_{0,BVI}$
(1)	(2)	(3)	(4)	(5)	(6)
LMC	-0.35	+0.01±0.15	-0.01±0.08	+0.00±0.08	+0.00±0.10
SMC	-0.70	+0.78±0.20	+0.49±0.14	+0.58±0.14	+0.68±0.16
SMC _{cor} ¹	-0.70	~+0.57	~+0.53	~+0.54	~+0.56

Table 6. Differences among LMC-relative absolute distance moduli for LMC and SMC fundamental Cepheids with $P \geq 6$ days. The last two lines give the observed variations between SMC and LMC variables and the predicted values for $\Delta[\text{Fe}/\text{H}]=-0.35$ according to the B -values listed in Table 4.

Galaxy	$\Delta\mu_{0,BV-VI}$	$\Delta\mu_{0,BV-BI}$	$\Delta\mu_{0,BV-BVI}$	$\Delta\mu_{0,BI-VI}$	$\Delta\mu_{0,BVI-VI}$	$\Delta\mu_{0,BVI-BI}$
(1)	(2)	(3)	(4)	(5)	(6)	(7)
LMC	+0.03±0.15	+0.01±0.11	+0.01±0.06	+0.02±0.04	+0.02±0.09	+0.00±0.05
SMC	+0.33±0.19	+0.23±0.14	+0.13±0.08	+0.09±0.05	+0.20±0.12	+0.10±0.07
SMC-LMC	~+0.30	~+0.22	~+0.12	~+0.07	~+0.18	~+0.10
$\Delta[\text{Fe}/\text{H}]=-0.35$	~+0.21	~+0.16	~+0.08	~+0.05	~+0.13	~+0.08

Table 7. Average LMC-relative absolute distance moduli for NGC 4258 Cepheids with $\rho/\rho_0 < 0.7$ (sample A) and $\rho/\rho_0 > 1.0$ (sample B).

Sample	$\langle \rho/\rho_0 \rangle$	[O/H] ^a	$\delta\mu_{0,BV}$	$\delta\mu_{0,VI}$	$\delta\mu_{0,BI}$	$\delta\mu_{0,BVI}$
(1)	(2)	(3)	(4)	(5)	(6)	(7)
A	0.40±0.22	+0.13±0.08	10.69±0.25	10.62±0.23	10.65±0.20	10.67±0.20
B	1.40±0.24	-0.37±0.09	10.94±0.25	10.85±0.12	10.88±0.12	10.90±0.17

^aBased on the Za94 oxygen gradient.

Table 8. Averaged differences among LMC-relative absolute distance moduli for NGC 4258 Cepheids with $\rho/\rho_0 < 0.7$ (sample A) and $\rho/\rho_0 < 1.0$ (sample B), in comparison with Magellanic and metal-rich Milky Way (MW) variables.

Sample (1)	$[O/H]$ (2)	$\Delta\delta\mu_{0,BV-VI}$ (3)	$\Delta\delta\mu_{0,BV-BI}$ (4)	$\Delta\delta\mu_{0,BV-BVI}$ (5)	$\Delta\delta\mu_{0,BI-VI}$ (6)	$\Delta\delta\mu_{0,BVI-VI}$ (7)	$\Delta\delta\mu_{0,BVI-BI}$ (8)
A	$+0.13\pm 0.08^a$	$+0.07\pm 0.28$	$+0.04\pm 0.21$	$+0.03\pm 0.11$	$+0.03\pm 0.08$	$+0.04\pm 0.17$	$+0.01\pm 0.10$
B	-0.37 ± 0.09^a	$+0.09\pm 0.24$	$+0.06\pm 0.18$	$+0.04\pm 0.10$	$+0.03\pm 0.07$	$+0.05\pm 0.15$	$+0.02\pm 0.08$
SMC	-0.88 ± 0.08^b	$+0.31\pm 0.17$	$+0.21\pm 0.14$	$+0.13\pm 0.07$	$+0.09\pm 0.05$	$+0.19\pm 0.11$	$+0.10\pm 0.07$
LMC	-0.37 ± 0.15^b	$+0.03\pm 0.15$	$+0.01\pm 0.11$	$+0.01\pm 0.06$	$+0.02\pm 0.04$	$+0.02\pm 0.09$	$+0.00\pm 0.05$
MW	$+0.15\pm 0.06^c$	-0.13 ± 0.12	-0.12 ± 0.10	-0.05 ± 0.05	-0.01 ± 0.04	-0.07 ± 0.08	-0.06 ± 0.05

^aZa94 oxygen gradient.

^bFerrarese et al. (2000)

^cGalactic Cepheids with $[Fe/H]_A=0.1-0.3$, and by adopting $[O/H] = [Fe/H]$

Table 9. TRGB and Cepheid distances determined by Sakai et al. (2004, [S04]) and by Rizzi et al. (2007, [R07]).

Galaxy	$12 + \log(O/H)$ (Za94)	μ_0 (TRGB) (R07)	$\mu_{0,VI}$ (Cep) (S04)	μ_0 (TRGB) (S04)
LMC	8.50	18.59±0.09	18.50±0.10	18.57±0.06
SMC	7.98	18.99±0.08	18.99±0.15 ¹	18.98±0.06
IC1613	7.86	24.31±0.06	24.17±0.33	24.38±0.05
IC4182	8.40	28.25±0.06	28.35±0.06	28.23±0.05
NGC224	8.98	24.47±0.11	24.38±0.05	24.37±0.08
NGC300	8.35	26.65±0.07	26.53±0.05	26.48±0.04
NGC598	8.82	24.81±0.04	24.47±0.11	24.71±0.06
NGC3109	8.06	25.52±0.05	25.54±0.28	25.57±0.05
NGC3351	9.24	30.39±0.13	29.92±0.09	29.92±0.05
NGC3621	8.75	29.36±0.11	29.15±0.06	29.26±0.12
NGC3031	8.75	28.03±0.12	27.75±0.08	27.70±0.04
NGC4258 _i	8.93	29.46±0.11	29.12±0.23 ^a	29.42±0.06 ^b
NGC4258 _o	8.53	29.46±0.11	29.35±0.12 ^a	29.42±0.06 ^b
NGC5253	8.15	27.88±0.11	27.63±0.14	99.00±0.00
NGC5457 _i	9.20	29.42±0.11	28.93±0.11	29.34±0.09
NGC5457 _o	8.50	29.42±0.11	29.24±0.08	29.34±0.09
NGC6822	8.14	23.37±0.07	23.30±0.07	99.00±0.00
SexA	7.49	25.67±0.13	25.66±0.14	25.78±0.06
SexB	7.56	25.63±0.04	25.63±0.09	25.79±0.04
WLM	7.74	24.77±0.09	25.01±0.10 ^c	24.93±0.04

^aThis paper.

^bMacri et al. (2006).

^cPietrzynski et al. (2007).